Patterns of speciation and parallel genetic evolution under adaptation from standing variation

Ken A. Thompson[1,2], Matthew M. Osmond[2] and Dolph Schluter[2]

[1]Corresponding author. Ken Thompson, email: kthomp1063@gmail.com

[2]Biodiversity Research Centre and Department of Zoology, University of British Columbia, Vancouver, Canada

Article type: Letter

Running title: Parallelism and speciation from standing variation

Keywords: Fisher's geometric model; ecological speciation; mutation-order speciation; numerical theory; simulation

Total word count: 4758

Abstract (244 Words)

When isolated populations adapt to novel environments, they may do so using the same or different alleles. Use of the same alleles—parallel genetic evolution—is increasingly likely if populations have shared ancestral standing genetic variation. Here, we investigate the conditions under which populations undergo parallel genetic evolution from standing variation and the associated implications for speciation via environment-specific hybrid fitness. Using computer simulations, we find that populations adapting to identical environments tend to fix the same alleles from standing variation unless there is a deficient or excess amount of variation in the founding population. We also find that the degree of parallel genetic adaptation decreases faster-than-linearly as selection deviates from fully parallel toward divergent. This rapid decrease in parallelism occurs because seemingly small environmental differences among populations correspond to steep reductions in the fraction of alleles that are mutually beneficial. Lastly, we show that adaptation from standing variation reduces the phenotypic segregation variance of hybrids under both parallel and divergent selection. Under parallel selection, parental populations fix the same alleles which do not segregate in hybrids. In addition, adaptation from standing variation proceeds via a greater number of alleles with individually smaller effects than when adaptation is from new mutation—this further reduces segregation variance even under divergent selection. This reduced segregation variance improves mean hybrid fitness when parents adapt to similar environments but reduces mean hybrid fitness under divergent adaptation. Therefore adaptation from standing variation forestalls speciation via parallel selection and promotes speciation via divergent selection.

41 **Impact summary**

42 Among all of the questions that evolutionary biologists have posed, some of the most lingering
43 concern the predictability of evolution. For example, if two groups of organisms independently
44 evolve similar traits in similar habitats, is it likely that this evolution proceeded using the same
45 genes? If so, what can we learn about the probability that these groups have evolved
46 reproductive barriers causing them to become distinct species? We investigate these two
47 questions from a theoretical perspective in our article and focus on the viability of hybrids as
48 measured in the environments to which their parents are adapted. In particular, we investigate
49 the role of standing genetic variation—the genetic variability that exists within a population at
50 any given time—in causing populations to evolve using the same genes. We have three main
51 conclusions. First, we find that the greatest parallel evolution results when there is a match
52 between the quantity of standing genetic variation and the selective demands of the
53 environment, and significant redundancy in the standing variation readily leads to non-
54 parallelism. Our second conclusion is that parallel evolution from standing genetic variation is
55 likely only when different populations adapt to very similar environments; small environmental
56 differences largely preclude parallelism at the genetic level. Finally, whereas standing genetic
57 variation decreases the likelihood of speciation when two populations adapt to similar
58 environments, it increases the likelihood of speciation when populations adapt to different
59 environments. In sum, our article indicates that adaptation from standing variation can have an
60 important role for speciation that depends on whether populations adapt to similar or different
61 environments.
62

Introduction

The process of adaptation involves positive natural selection on beneficial alleles that improve the fit of a population to its environment. Adaptation can proceed via selection on new mutations or on pre-existing standing genetic variation (Orr and Betancourt 2001). If populations experience divergent natural selection, which favours distinct phenotypes in different environments, then different alleles are expected to fix regardless of their origin. Parallel natural selection, by contrast, favours the same phenotypes and alleles in different populations. Under parallel selection, distinct populations might experience and fix alternative adaptive alleles by chance (Mani and Clarke 1990), but the probability of genetic parallelism is expected to be greater if populations share a common pool of ancestral standing variation (Schluter and Conte 2009; Conte et al. 2012). Here, we investigate how the availability of standing genetic variation for adaptation affects parallel genetic evolution—defined as reuse of the same alleles during independent bouts of adaptation—and the associated implications for speciation via reduced hybrid fitness.

Adaptation facilitates progress towards speciation when adapting populations evolve reproductive isolating barriers as a by-product. One reason these reproductive isolating barriers can arise is because genetic differences between populations reduce the fitness of their hybrids, thereby reducing gene flow upon secondary contact. Under ecological speciation driven by divergent selection (Schluter 1996), F_1 hybrids might be intermediate in phenotype and unfit in both parental environments (e.g., Hatfield and Schluter 1999). Under an alternative process, populations diverge genetically by chance in the course of adapting to similar environments despite parallel natural selection ('mutation-order' speciation; Schluter 2009). In

this case, distinct populations fix different adaptive alleles that—when combined—render hybrids less fit than either parent because they have novel phenotypes poorly suited to the parental environment. A central goal of research on speciation is to characterize the conditions that can facilitate and impede progress toward ecological and mutation-order speciation.

Adaptation from standing variation is common and is responsible for some of the most spectacular adaptive radiations found in nature (e.g., African cichlids; Brawand et al. 2015). Nevertheless, the implications of standing variation for the process of speciation have not been explored. We hypothesized that—besides speeding up the process—adaptation from standing variation would reduce the evolution of reproductive isolation under parallel selection because adapting populations would fix the same alleles and therefore fewer incompatibilities. We also hypothesized that standing variation would have less of an effect on genetic parallelism and the evolution of isolating barriers under divergent selection.

In this article, we address the following question: Under what conditions do populations undergo parallel genetic adaptation from standing variation and what are the associated implications for the evolution of reproductive isolation between them? We note that 'divergent' and 'parallel' natural selection—and their corollaries of ecological and mutation-order speciation—are useful concepts but are the endpoints of a continuum of possible environmental differences (Langerhans and Riesch 2013; Martin and Lenormand 2015; Stuart et al. 2017; Bolnick et al. 2018). Few theoretical studies have investigated patterns of parallel genetic evolution and speciation across environments of varying similarity, and our focus is largely on determining how patterns change across the continuum of parallel to divergent. We use individual-based simulations to investigate our research question and include analytical

107 derivations to explain simulation results where relevant. Our results suggest that standing
108 variation has important implications for speciation that vary across environments.
109
110 **Methods**
111 We used computer simulations to investigate parallel genetic adaptation and speciation from
112 ancestral standing variation. Our simulations were carried out using the conceptual framework
113 of Fisher's (1930) geometric model of adaptation (reviewed by Tenaillon [2014]). Fisher's model
114 makes explicit and testable predictions that have received support in laboratory and field
115 studies (MacLean et al. 2010; Rogers et al. 2012; Stearns and Fenster 2016). While originally
116 developed to make inferences about the genetics of adaptation, the model has been adapted
117 to study the evolutionary genetics of speciation (Barton 2001; Chevin et al. 2014; Fraïsse et al.
118 2016; Simon et al. 2017). We considered the case of a single ancestral population that founds
119 two identical populations in novel environments, which then adapt without gene flow between
120 them (i.e., allopatry; see Fig. 1A). After adaptation, populations are brought into secondary
121 contact. This general colonization history is modelled around the process of adaptation as it can
122 occur in nature, for example in insects with respect to their host-plants ('micro-allopatry', e.g.,
123 Drès and Mallet 2002), fish populations in post-glacial lakes (Bell and Foster 1994) and in birds
124 or plants isolated within glacial refugia (e.g., Weir and Schluter 2004; Pettengill and Moeller
125 2012).
126
127 *Genotype to phenotype*

The phenotype of a haploid individual is represented by an m-dimensional vector, $\boldsymbol{z} = [z_1, z_2, \ldots, z_m]$, with m being the number of independent 'traits' (Orr 2000). Each trait value, z_i, is determined by the summed effects of all underlying loci, which are initially fixed for alleles with an effect of 0 on all m traits. We focus on $m = 2$ in our numerical analyses, and present analytical derivations in higher dimensions in the relevant contexts to investigate how trait dimensionality (i.e., 'organism complexity'; Orr 2000) affects our conclusions.

Life-cycle

We assume non-overlapping generations. Viability selection occurs at the beginning of each generation, during the haploid phase. The probability that an individual with phenotype $\boldsymbol{z}$ survives is a Gaussian function of its Euclidean distance from the optimum, $||\boldsymbol{z} - \boldsymbol{o}||$, and the strength of selection, $\boldsymbol{s}$: $P = \exp(-s||\boldsymbol{z} - \mathbf{o}||^2/2)$ (equation 1; Fraïsse et al. [2016]). We note that some empirical studies support the use of Gaussian fitness functions (e.g., Martin and Lenormand [2006]). The simulation is ended if no individuals survive. If the number of survivors exceeds the carrying capacity, K, then survivors are randomly culled to a population size of K.

Haploids that survive viability selection then randomly conjugate (each with any individual but itself; i.e., self-incompatible) and undergo meiosis with free recombination between all loci. Each mating pair is a diploid individual that generates $2B$ haploid offspring, which each acquire a new mutation with probability μ. An infinite number of loci is assumed, such that each mutation arises at a new locus ('infinite-sites' *sensu* Kimura [1969]). For simplicity we assume that the effect of a mutation on each of the m traits is independently drawn from a normal distribution with a mean of 0 and SD of σ. Thus all mutations are unique

('continuum-of-alleles' *sensu* Kimura [1965]). The effects of mutational covariance and modularity (restricted pleiotropy *sensu* Chevin et al. [2010]) are left out but could be readily explored with the provided simulation code (**Data accessibility**). See Table 1 for descriptions of all parameters and values used in simulations.

Generating ancestral standing genetic variation

We initiate focal populations with standing genetic variation from a common ancestor. To generate ancestral standing variation, we conducted burn-in simulations of a large population (K_{anc} = 10,000) under weak stabilizing selection (s_{anc} = 0.01) at the origin ($\boldsymbol{o}_{anc}$ = [0, 0, … 0]) for 100,000 generations. All other parameters (e.g., mutation rate) were identical to adapting populations (Table 1). Ancestral populations reached mutation-selection balance and had, on average, a mean of 192 segregating alleles (Fig. S1A). Each segregating allele was present in, on average, 7.3 % of individuals (Fig. S1B).

Adaptation to a new environment

Following the burn-in we generated two initially-identical founder (i.e., parental) populations. The founder population size was equal to the carrying capacity (here 1000 individuals). Founder populations were fixed for alleles that were fixed in the ancestor, and the amount of standing variation was determined by sampling *n* segregating alleles from the ancestor. Populations adapted from only new mutation when *n* = 0 and otherwise contained some ancestral standing variation. Each of the *n* segregating alleles were selected for inclusion in the founder populations with a probability proportional to their frequency in the ancestor, and the expected

172 frequency of an allele in a founding population was equal to its frequency in the ancestor.
173 Specifically, each founding individual inherited a particular allele with a probability equal to its
174 frequency in the ancestor. For each parameter combination, we began each simulation from a
175 unique realization of the ancestor (i.e., distinct burn-in). This randomly generated population
176 was duplicated and used to found both adapting populations.

177 After initialization, founder populations adapted to their respective specified phenotypic
178 optima without any gene flow (Fig. 1B). Adaptation proceeded via the reassortment of
179 ancestral standing variation (if $n > 0$) and via new mutation (probability of mutation, $\mu = 0.001$;
180 all simulations) simultaneously. Individuals gain new mutations with identical probability and
181 properties as in the ancestor. There are two key features of the new phenotypic optima. The
182 first is the initial distance to the optima, calculated as the Euclidean distance between the
183 optima and the origin, d. More distant optima require a greater amount of phenotypic change
184 and initially exert stronger selection. The second key feature is the angle of divergence, Θ,
185 which captures the difference in direction from the origin to the optima of the two populations
186 (see Fig. 1B). Angle is used to describe the continuum of parallel to non-parallel evolution and is
187 explicitly invoked in most metrics that quantify phenotypic parallelism (see Bolnick et al.
188 [2018]). Optima differing by a small angle impose relatively parallel natural selection on
189 founder populations, whereas optima whose direction differ by large angles impose divergent
190 selection.

191 We ended simulations after 2000 generations, at which time all populations had
192 reached their phenotypic optima (Fig. S2A) and mutation-selection balance (Fig. S2B). An
193 unavoidable and important effect of standing variation is that it quickens adaptation because

194 populations do not have to 'wait' for beneficial mutations to arise (Barrett and Schluter 2008).
195 In our model and others like it (e.g., Barton [2001] & Chevin et al. [2014]), reproductive
196 isolation evolves rapidly during the initial stages of adaptation and then decelerates as
197 populations approach their optima. Accordingly, any reduction in hybrid fitness that evolves
198 does so more rapidly when evolution occurs from standing variation. We allowed sufficient
199 time in our simulations for all populations to reach their optima even when adaptation is from
200 only new mutation. Populations continue to diverge indefinitely after reaching their optima, but
201 this divergence is weak and constant across all simulations in our study. Therefore, our
202 conclusions refer to equilibrium conditions rather than transient states and are unaffected by
203 standing variation's influence on the speed of adaptation.
204
205 *Formation of hybrids and quantification of segregation variance & fitness*
206 After the adaptation phase of simulations had ended, derived populations 'met' in secondary
207 contact and produced hybrids. We randomly chose a haploid individual from each of the two
208 populations to form a diploid (F_1) that produce recombinant haploid hybrids through meiosis
209 with free recombination among loci. If an allele was shared by both parents—which is possible
210 only if it originated from the ancestral standing variation because new mutations are unique
211 and thus cannot arise de novo in both populations—then the allele was present in the hybrid.
212 Alleles present in only one parent—all alleles arising from new mutation during adaptation and
213 alternative alleles fixed from the standing variation—were inherited by the hybrid offspring
214 with probability 0.5 (i.e., fair Mendelian segregation). This process was repeated to create 100
215 hybrids between the pair of parental populations.

We calculated two quantities of interest in the hybrids: segregation variance and fitness. Segregation variance is the phenotypic variation of hybrids (Wright 1968; Slatkin and Lande 1994) and is calculated here as the mean phenotypic variance across all *m* traits. Higher segregation variance results when parents are differentiated by a greater number of alternative alleles (holding effect size constant) or alleles of individually-larger effect (holding number of alleles constant) (Slatkin and Lande 1994; Chevin et al. 2014). Segregation variance captures the phenotypic consequences of hybridization and is therefore more biologically meaningful than simply quantifying the number of different alleles that distinguish populations or their average effect size. Phenotypic variance in parental populations before hybridization is near zero and is not affected by the quantity of standing variation nor the initial distance to the optimum (Fig. S2C).

An individual hybrid's fitness in a given parental environment was calculated from its phenotype in the same manner as the fitness of their parents (Fig. 1C). We quantified the fitness of each hybrid in both parental environments and recorded its final fitness as the larger of the two values. That is, we calculated the survival probability (equation 1) of each hybrid with respect to both optima, and an individual hybrid's survival probability was the higher of the two values. This can be imagined as, for example, giving the hybrid a choice of alternative host-plants (Drès and Mallet 2002). Our fitness metric reflects that which is traditionally recognized as 'extrinsic' isolation, and explicitly considers epistasis for fitness between alleles at different loci. Accordingly, two alleles that reduce fitness when combined in a hybrid can be considered Bateson-Dobzhansky-Muller incompatibility loci (Bateson 1909; Dobzhansky 1937; Muller 1942; Chevin et al. 2014; Fraïsse et al. 2016) with environment-specific effects on fitness

238 (see Arnegard et al. [2014], Schumer et al. [2014], and Ono et al. [2017] for discussion of
239 environment-specific incompatibilities).
240
241 **Results and discussion**
242 *Effects of standing variation on the segregation variance in hybrids following parallel and*
243 *divergent selection*
244 We first investigated how the quantity of standing variation in the founding populations affects
245 the segregation variance in hybrids (hereafter simply 'segregation variance'). To investigate
246 these dynamics, we ran simulations in which populations underwent either parallel (identical
247 optima, $\Theta = 0°$) or divergent (opposite optima, $\Theta = 180°$) evolution, and repeated this with
248 different amounts of ancestral standing variation (via n). A representative set of simulations is
249 plotted in Figure 2A.
250 Several conclusions emerge from these simulations. First, segregation variance is
251 consistently high when populations undergo divergent ($\Theta = 180°$) adaptation. This is because
252 alleles that are beneficial in one environment are deleterious in the other. Thus populations fix
253 alternative adaptive alleles regardless of whether they originate in the standing variation or
254 arise from new mutation. This is true for any dimensionality, m. Second, under parallel
255 evolution ($\Theta = 0°$), standing variation generally reduces segregation variance. This is largely
256 because the same alleles are fixed in both populations and therefore do not segregate in
257 hybrids. Third, segregation variance under parallel selection is minimized when populations are
258 founded with intermediate quantities of standing variation. When there is little or no standing
259 variation, populations undergo non-parallel genetic evolution due to their reliance on

alternative new mutations. When there is substantial standing variation, there are many redundant alleles in the standing variation and populations again fix alternative beneficial variants. The quantity of standing variation that minimizes segregation variance under parallel selection (arrow in Fig. 2A) is greater for more distant optima (Fig. 2B) because a greater number of mutations are required for adaptation.

It has been widely suggested in the literature that parallel genetic evolution is most likely when populations are founded from a common ancestor with the same pool of standing variation (Conte et al. 2012). Our results largely confirm this intuition because the simulations indicate that the populations adapted using the same alleles under parallel selection. For maximal parallel evolution, however, there must be a match between the supplied standing variation and the demands of the environment. Significant redundancy in the standing variation can lead to non-parallel genetic evolution from standing variation even when optima are identical.

Parallel genetic evolution across environments

To investigate the relationship between the angle of divergence (i.e., Θ) and segregation variance, we conducted simulations across a range of angles between 0° and 180°. In this section, simulations had either no standing variation (i.e., only *de novo* mutation) or the amount of standing variation that minimized segregation variance under parallel selection (Θ = 0°; arrow in Fig. 2A). We plot a representative set of simulations in Figure 3A.

Several key results emerge from these simulations. First, segregation variance is not affected by the angle of divergence when there is no standing variation (n = 0 in Fig. 2; light

green line and points in Fig. 3A). This occurs because all new mutations are unique and arise at different loci in our simulations. Second, when there is standing variation, segregation variance increases faster-than-linearly with the angle of divergence (compare dark green and black lines in Fig. 3A). This result is partially caused by the specific geometric properties of angles: a given change in Θ causes a larger change in the Euclidean distance between optima, δ, when Θ is smaller (Fig. S3A; see also Fig. S3B for same data as in Fig. 3A plotted with δ on x-axis) than when Θ is large.

The geometric properties of adaptation also contribute to the rapid decrease in genetic parallelism as the angle of divergence increases. During adaptation, a given mutation is only expected to fix in two allopatric populations if it is beneficial in both. For a given population, beneficial mutations bring populations closer to the centre of a hypersphere (circle when $m = 2$) centered at the optimum with the adapting population a point on the surface (Fisher 1930; see cartoon inset of Fig. 3B). The radius of the hypersphere is equivalent to the initial distance to the optimum, d. Considering two populations, a given mutation is mutually beneficial if it its phenotypic effect brings a population's phenotype into in the intersecting volume of the two hyperspheres (pink region in Fig. 3B inset). The expected degree of non-parallelism is therefore captured by the fraction of mutations that are beneficial in one population but deleterious in the other (e.g., for 'red' population in Fig 3B inset: area of the red region divided by the area of the pink and red regions combined). That is, the alleles favoured by selection in only one of two populations are those with phenotypic effects leading into the *non-overlapping* regions of the hyperspheres. Analytically (see **Appendix**), we show that this 'fraction of non-overlap' is zero when $\Theta = 0°$, one when $\Theta = 180°$, and increases faster-than-linearly with Θ (Fig. 3B; see also Fig.

S3A for the relationship between Θ, δ, and the fraction of non-overlap). This fraction of non-overlap increases even more rapidly with Θ in higher dimensions (compare solid line to dashed in Fig. 3B). Because the fraction of non-overlap is independent of the distance to an optimum (see **Appendix**), this pattern is expected to remain constant over the course of an adaptive 'walk' (*sensu* Orr [1998]) and regardless of whether populations have the same or different initial phenotype.

In addition, the average probability of fixation for mutually beneficial mutations decreases with the angle of divergence. This is intuitive: when $\Theta = 0°$, the region of overlap contains mutations that are highly beneficial in both populations (e.g., their shared optima). As Θ increases, the mutations remaining in the region of overlap have more deleterious pleiotropic consequences and are thus less mutually beneficial.

We note that the above arguments reflect the probability of parallel genetic evolution generally and not from standing variation specifically. Therefore, populations adapting to similar environments have a higher probability of fixing similar mutations whether the mutations arise *de novo* or were segregating in the ancestor. The arguments above are thus component pieces of a comprehensive theory of the probability of genetic parallelism across environments during adaptation without gene flow. Integrating the processes discussed above with estimates of both the distribution of fitness effects of new mutations (Eyre-Walker and Keightley 2007) and the fitness effects of mutations across environments (Martin and Lenormand 2015) will be valuable.

The simulations depicted in Fig. 3 also illustrate an unanticipated general effect of standing variation: a reduction of segregation variance for all angles of divergence. This is most

apparent by examining the right side of Fig. 3A. When selection is divergent, Θ = 180°, there are no beneficial alleles shared between adapting populations, yet segregation variance is lower than when adaptation occurs only by new mutations. The reason standing variation reduces segregation variance in our simulations is that past stabilizing selection in the ancestor changes the effect sizes of alleles during adaptation by removing large effect mutations (see Fig. 1C). Supporting this hypothesis, we conducted a separate set of simulations initiated with standing variation but without past selection and found that segregation variance under divergent selection was the same as when adaptation was from new mutation only (Fig. S4). In the absence of large-effect mutations, adaptation from standing genetic variation proceeds via a greater number of alleles of relatively small effect compared to adaptation from new mutation. This, in turn, reduces segregation variance because individuals recover a more intermediate phenotype as a greater number of smaller effect alleles contribute to character divergence (Castle 1921; Barton et al. 2017). In addition to past selection removing large-effect alleles, small-effect alleles are more likely to be used in adaptation when present in the standing variation because they are less likely to be lost due to drift (Orr and Betancourt 2001; Hermisson and Pennings 2005). Large-effect alleles are more costly when dimensionality is greater (Orr 2000) and therefore small-effect alleles in the standing variation should further reduce segregation variance in higher dimensions.

Effect of standing variation on environment-specific hybrid fitness

In this section, we use data from the simulations in the previous section (see Fig. 3A) to evaluate the effect of standing variation on hybrid fitness. Specifically, we focus on differences

in mean hybrid fitness between simulations that were initiated with and without standing variation. For an individual simulation, mean relative hybrid fitness was calculated as: [mean probability of an individual hybrid surviving] / [probability of an individual parent surviving]. The results of these simulations with respect to mean fitness are plotted in Figures 4 A & B.

The simulations reveal that standing genetic variation improves mean hybrid fitness when parental populations adapt to similar optima, but reduces hybrid fitness when parents undergo divergent adaptation. This result is caused by environment-specific effects of segregation variance on hybrid fitness (Fig. 4C). When the hybrid phenotype distribution is centred at the phenotypic optimum, as it is under parallel selection (i.e., $\Theta = 0°$), segregation variance is deleterious and the use of shared standing variation causes hybrids to have uniform phenotypes that resemble both parents. By contrast, when selection is divergent hybrids fall in a fitness valley between parental optima and some segregation variance is beneficial for mean hybrid fitness. This is because phenotypic variation in hybrids causes some individuals on the tails of the phenotype distribution to approach an optimum (see Fig. 1C). (Maximum hybrid fitness is not affected by standing variation under parallel selection and is reduced by standing variation under divergent selection [Fig. S5]).

These results indicate that, relative to when adaptation is from only new mutation, the effect of standing variation is to forestall the accumulation of reproductive isolation in response to parallel natural selection and facilitate the evolution of reproductive isolation in response to divergent natural selection. Standing variation necessarily speeds up adaptation (Fig. S2; see also Fig. S6 for plots of segregation variance over time) and so by necessity the evolution of isolating barriers occurs more quickly. Our conclusions about the effects of standing variation

on hybrid fitness are reported at mutation-selection balance when populations are locally-adapted. Therefore our results may not hold for cases where populations are still experiencing strong selection in their new environment. Our conclusions about mutation-order speciation do not change in higher dimensions. Under divergent selection, however, the amount of segregation variance that maximizes mean hybrid fitness declines as dimensionality increases because the number of ways hybrids can 'go wrong' (Orr 2000) increases (see online Mathematica notebooks for approximations in higher dimensions for mean hybrid fitness under parallel and divergent selection). Maximum hybrid fitness, by contrast, always increases with higher segregation variance under divergent selection.

Additional factors influencing the probability of parallel genetic evolution

Several processes that we did not model could affect the probability of parallel genetic evolution and the evolution of hybrid fitness. First, we assumed there was no recurrent mutation at the same locus (e.g., Chan et al. 2010). Recurrent mutation would not qualitatively change our results but would increase genetic parallelism even without standing variation. Second, we assumed no gene flow between populations. Gene flow is expected to reduce the likelihood that populations fix alternative alleles under parallel natural selection (Nosil and Flaxman 2011; Anderson and Harmon 2014) and also impede local adaptation in response to divergent selection (Nosil 2012). Third, we assume that the ancestral standing variation is random with respect to the new environment. In some cases, however, alleles that are beneficial in a particular derived habitat may seed into—and be maintained within—the ancestral population via a balance between regular introgression and selection (Schluter and

Conte 2009). Such variants could be maintained at a higher frequency in the ancestral populations than those maintained by mutation selection balance. When founders bring such variation to a new environment that is similar to that of the source populations, the effects of such 'transported' alleles are no longer random with respect to the direction of selection but instead are highly likely to be beneficial and evolve in parallel (see Nelson and Cresko 2018).

Fourth, we assumed that distinct populations were founded from the same ancestor and hence had access to an identical pool of standing variation. If the ancestral population is structured, such that new populations are founded with different subsets of ancestral standing variation, we expect reduced genetic parallelism under parallel selection compared to the case where founder populations are identical (Conte et al. 2015). Differences in allele frequencies between ancestral populations also reduces parallel genetic evolution because for a given effect size mutations at highest frequencies are most likely to be used for adaptation (MacPherson and Nuismer 2017). Founder events are therefore expected to lead to greater genetic divergence between populations undergoing parallel natural selection.

The interpretation of our simulation results has several additional caveats. In particular, we considered only haploid selection and strict additivity of allelic effects on phenotypes—future work should investigate the effects of ploidy on parallel genetic evolution and on speciation from standing variation. We also assumed that the sole fitness optima available to hybrids are those that the two parents are adapted to. Hybrids often perform best when there is an additional adaptive peak not being exploited by the parental forms (Rieseberg et al. 1999). Last, we only considered environment-specific hybrid fitness rather than 'intrinsic' isolating barriers. Intrinsic isolating barriers are a function of genetic divergence among populations (Orr

414 1995). Since segregation variance in our study directly reflects genetic divergence between
415 populations, our results of segregation variance across environments (Fig. 3) could have
416 implications for the evolution of intrinsic barriers.
417
418 *Implications for studies of parallel evolution*
419 Our results predict that subtle differences in the environments to which populations are
420 adapting can substantially preclude parallel genetic evolution. This is because seemingly small
421 differences in habitat similarity (via Θ) greatly reduce the quantity of alleles that are expected
422 to be beneficial in both populations. Even for cases termed 'parallel', there can be a wide range
423 of phenotypic variation among replicates (for quantitative summary in fishes see Oke et al.
424 2017). If researchers wrongly assume that environments or phenotypes are similar or even
425 identical, they may be misled into attributing genetic non-parallelism to various biological
426 mechanisms when a better explanation is that the allele is not mutually beneficial. This rapid
427 loss of shared beneficial alleles is especially pronounced for cases with high dimensionality.
428 Dimensionality is difficult to quantify but estimates are typically between 1 and 10 for bacteria
429 (Tenaillon 2014). In complex organisms (e.g., vertebrates) dimensionality is expected to be
430 higher and therefore genetic parallelism should be less common.
431
432 *Conclusion*
433 Our analyses confirm the intuition that allopatric populations adapting from a common pool of
434 ancestral standing genetic variation tend to undergo parallel genetic evolution in response to
435 parallel natural selection. We show that the probability of parallel genetic evolution rapidly

436 decreases as selection tends from parallel toward divergent and that this reduction in genetic
437 parallelism occurs most quickly in complex organisms. Parallel genetic adaptation from standing
438 variation reduces the segregation variance of hybrids under parallel selection. We also find that
439 adaptation from standing variation leads to reduced segregation variance regardless of the
440 angle of divergence because adaptation proceeds via more alleles of individually smaller effect.
441 This reduced segregation variance further improves mean hybrid fitness under parallel natural
442 selection but reduces mean hybrid fitness under divergent selection. In sum, adaptation from
443 standing genetic variation can affect the evolution of reproductive isolating barriers under both
444 parallel and divergent natural selection and this is mediated by its effects on the segregation
445 variance of hybrids.
446

447 **Acknowledgements**

448 Discussions with S. Otto motivated and refined the approach used in this study. Feedback from
449 S. Arnold, M. Chapuisat, L. Chavarie, R. Holzman, A. MacPherson, S. Otto, L. Rieseberg, J.
450 Rolland, M. Urquhart-Cronish and R. Yamaguchi improved the manuscript. K.A.T. was funded by
451 The University of British Columbia, the Natural Sciences and Engineering Research Council of
452 Canada (NSERC) and the Izaak Walton Killam Memorial Fund for Advanced Studies. M.M.O. was
453 funded by The University of British Columbia. D.S. was funded by the Canada Foundation for
454 Innovation, Genome BC, and NSERC.
455

456 **Author contributions**

457 K.A.T. and D.S. developed the original ideas upon which the paper is based. K.A.T. wrote the
458 first draft of the manuscript with input from M.M.O. and D.S., and all authors contributed to
459 subsequent revisions. M.M.O. wrote the simulations and analytical derivations with input from
460 K.A.T.. K.A.T. performed, optimized, and analyzed the simulations, with input from M.M.O.
461
462 **Data accessibility**
463 Python (version 3.6.1) scripts and resulting data, R (version 3.4.1) scripts to process and plot the
464 simulated data, and a Mathematica notebook (version 9; and PDF copy) to derive analytical
465 results will be archived on Dryad. For now, these are hosted on GitHub
466 (https://github.com/Ken-A-Thompson/SVS).

467 **References**

468 Abramowitz, M., and I. A. Stegun. 1972. Handbook of mathematical functions: with formulas,
469 graphs, and mathematical tables. United States Department of Commerce, Washington
470 DC, USA.

471 Anderson, C. J. R., and L. Harmon. 2014. Ecological and mutation-order speciation in digital
472 organisms. Am. Nat. 183:257–268.

473 Arnegard, M. E., M. D. McGee, B. Matthews, K. B. Marchinko, G. L. Conte, S. Kabir, N. Bedford,
474 S. Bergek, Y. F. Chan, F. C. Jones, D. M. Kingsley, C. L. Peichel, and D. Schluter. 2014.
475 Genetics of ecological divergence during speciation. Nature 511:307–311.

476 Barrett, R. D. H., and D. Schluter. 2008. Adaptation from standing genetic variation. Trends Ecol.
477 Evol. 23:38–44.

478 Barton, N. H. 2001. The role of hybridization in evolution. Mol. Ecol. 10:551–568.

479 Barton, N. H., A. M. Etheridge, and A. Véber. 2017. The infinitesimal model: Definition,
480 derivation, and implications. Theor. Popul. Biol. 118:50–73.

481 Bateson, W. 1909. Heredity and variation in modern lights. Pp. 85–101 *in* A. C. Seward, ed.
482 Darwin and Modern Science. Cambridge University Press, Cambridge.

483 Bell, M. A., and S. A. Foster. 1994. The Evolutionary Biology of the threespine stickleback.
484 Oxford University Press.

485 Bolnick, D. I., R. D. H. Barrett, K. B. Oke, D. J. Rennison, and Y. E. Stuart. 2018. (Non)Parallel
486 Evolution. Annu. Rev. Ecol. Evol. Syst. In press.

487 Brawand, D., C. E. Wagner, Y. I. Li, M. Malinsky, I. Keller, S. Fan, O. Simakov, A. Y. Ng, Z. W. Lim,
488 E. Bezault, J. Turner-Maier, J. Johnson, R. Alcazar, H. J. Noh, P. Russell, B. Aken, J. Alföldi, C.

Amemiya, N. Azzouzi, J. F. Baroiller, F. Barloy-Hubler, A. Berlin, R. Bloomquist, K. L. Carleton, M. A. Conte, H. D'Cotta, O. Eshel, L. Gaffney, F. Galibert, H. F. Gante, S. Gnerre, L. Greuter, R. Guyon, N. S. Haddad, W. Haerty, R. M. Harris, H. A. Hofmann, T. Hourlier, G. Hulata, D. B. Jaffe, M. Lara, A. P. Lee, I. MacCallum, S. Mwaiko, M. Nikaido, H. Nishihara, C. Ozouf-Costaz, D. J. Penman, D. Przybylski, M. Rakotomanga, S. C. P. Renn, F. J. Ribeiro, M. Ron, W. Salzburger, L. Sanchez-Pulido, M. E. Santos, S. Searle, T. Sharpe, R. Swofford, F. J. Tan, L. Williams, S. Young, S. Yin, N. Okada, T. D. Kocher, E. A. Miska, E. S. Lander, B. Venkatesh, R. D. Fernald, A. Meyer, C. P. Ponting, J. T. Streelman, K. Lindblad-Toh, O. Seehausen, and F. Di Palma. 2015. The genomic substrate for adaptive radiation in African cichlid fish. Nature 513:375–381.

Castle, W. E. 1921. An improved method of estimating the number of genetic factors concerned in cases of blending inheritance. Science 54:223.

Chan, Y. F., M. E. Marks, F. C. Jones, G. Villarreal, M. D. Shapiro, S. D. Brady, A. M. Southwick, D. M. Absher, J. Grimwood, J. Schmutz, R. M. Myers, D. Petrov, B. Jónsson, D. Schluter, M. A. Bell, and D. M. Kingsley. 2010. Adaptive evolution of pelvic reduction in sticklebacks by recurrent deletion of a *Pitx1* enhancer. Science 327:302–305.

Chevin, L. M., G. Decorzent, and T. Lenormand. 2014. Niche dimensionality and the genetics of ecological speciation. Evolution 68:1244–1256.

Chevin, L. M., G. Martin, and T. Lenormand. 2010. Fisher's model and the genomics of adaptation: Restricted pleiotropy, heterogenous mutation, and parallel evolution. Evolution 64:3213–3231.

Conte, G. L., M. E. Arnegard, J. Best, Y. F. Chan, F. C. Jones, D. M. Kingsley, D. Schluter, and C. L.

Peichel. 2015. Extent of QTL reuse during repeated phenotypic divergence of sympatric threespine stickleback. Genetics 201:1189–1200.

Conte, G. L., M. E. Arnegard, C. L. Peichel, and D. Schluter. 2012. The probability of genetic parallelism and convergence in natural populations. Proc. R. Soc. B Biol. Sci. 279:5039–5047.

Dobzhansky, T. 1937. Genetics and the origin of species. Columbia University Press, New York.

Drès, M., and J. Mallet. 2002. Host races in plant-feeding insects and their importance in sympatric speciation. Philos. Trans. R. Soc. B Biol. Sci. 357:471–492.

Eyre-Walker, A., and P. D. Keightley. 2007. The distribution of fitness effects of new mutations.

Fisher, R. F. 1930. The Genetical Theory of Natural Selection. Oxford University Press, Oxford, UK.

Fraïsse, C., P. A. Gunnarsson, D. Roze, N. Bierne, and J. J. Welch. 2016. The genetics of speciation: Insights from Fisher's geometric model. Evolution 70:1450–1464.

Hatfield, T., and D. Schluter. 1999. Ecological speciation in sticklebacks: environment-dependent hybrid fitness. Evolution 53:866–873.

Hermisson, J., and P. S. Pennings. 2005. Soft sweeps: Molecular population genetics of adaptation from standing genetic variation. Genetics 169:2335–2352.

Kimura, M. 1965. A stochastic model concerning the maintenance of genetic variability in quantitative characters. Proc. Natl. Acad. Sci. U. S. A. 54:731–736.

Kimura, M. 1969. The number of heterozygous nucleotide sites maintained in a finite population due to steady flux of mutations. Genetics 61:893–903.

Langerhans, R. B., and R. Riesch. 2013. Speciation by selection: A framework for understanding

533 ecology's role in speciation. Curr. Zool. 59:31–52.

534 Li, S. 2011. Concise formulas for the area and volume of a hyperspherical cap. Asian J. Math.

535 Stat. 4:66–70.

536 MacLean, R. C., G. G. Perron, and A. Gardner. 2010. Diminishing returns from beneficial

537 mutations and pervasive epistasis shape the fitness landscape for rifampicin resistance in

538 *Pseudomonas aeruginosa*. Genetics 186:1345–1354.

539 MacPherson, A., and S. L. Nuismer. 2017. The probability of parallel genetic evolution from

540 standing genetic variation. J. Evol. Biol. 30:326–337.

541 Mani, G. S., and B. C. Clarke. 1990. Mutational order: A major atochastic process in evolution.

542 Proc. R. Soc. B Biol. Sci. 240:29–37.

543 Martin, G., and T. Lenormand. 2006. The fitness effect of mutations across environments: a

544 survey in light of fitness landscape models. Evolution 60:2413–2427.

545 Martin, G., and T. Lenormand. 2015. The fitness effect of mutations across environments:

546 Fisher's geometrical model with multiple optima. Evolution 69:1433–1447.

547 Muller, H. J. 1942. Isolating mechanisms, evolution and temperature. Biol. Symp 6:71–125.

548 Nelson, T. C., and W. A. Cresko. 2018. Ancient genomic variation underlies repeated ecological

549 adaptation in young stickleback populations. Evol. Lett. 2:9–21.

550 Nosil, P. 2012. Ecological speciation. Oxford University Press, Oxford, UK.

551 Nosil, P., and S. M. Flaxman. 2011. Conditions for mutation-order speciation. Proc. R. Soc. B

552 Biol. Sci. 278:399–407.

553 Oke, K. B., G. Rolshausen, C. LeBlond, and A. P. Hendry. 2017. How parallel is parallel evolution?

554 A comparative analysis in fishes. Am. Nat. 190:1–16.

555 Ono, J., A. C. Gerstein, and S. P. Otto. 2017. Widespread genetic incompatibilities between first-
556 step mutations during parallel adaptation of *Saccharomyces cerevisiae* to a common
557 environment. PLoS Biol. 15:e1002591.
558 Orr, H. A. 2000. Adaptation and the cost of complexity. Evolution 54:13–20.
559 Orr, H. A. 1998. The population genetics of adaptation: The distribution of factors fixed during
560 adaptive evolution. Evolution 52:935.
561 Orr, H. A. 1995. The population genetics of speciation: The evolution of hybrid incompatibilities.
562 Genetics 139:1805–1813.
563 Orr, H. A., and A. J. Betancourt. 2001. Haldane's sieve and adaptation from the standing genetic
564 variation. Genetics 157:875–884.
565 Pettengill, J. B., and D. A. Moeller. 2012. Phylogeography of speciation: Allopatric divergence
566 and secondary contact between outcrossing and selfing *Clarkia*. Mol. Ecol. 21:4578–4592.
567 Rieseberg, L. H., M. a Archer, and R. K. Wayne. 1999. Transgressive segregation, adaptation and
568 speciation. Heredity 83:363–372.
569 Rogers, S. M., P. Tamkee, B. Summers, S. Balabahadra, M. Marks, D. M. Kingsley, and D.
570 Schluter. 2012. Genetic signature of adaptive peak shift in threespine stickleback.
571 Evolution 66:2439–2450.
572 Schluter, D. 1996. Ecological speciation in postglacial fishes. Philos. Trans. R. Soc. B Biol. Sci.
573 351:807–814.
574 Schluter, D. 2009. Evidence for ecological speciation and its alternative. Science 323:737–741.
575 Schluter, D., and G. L. Conte. 2009. Genetics and ecological speciation. Proc. Natl. Acad. Sci. USA
576 106.Sup1:9955–62.

577 Schumer, M., R. Cui, D. L. Powell, R. Dresner, G. G. Rosenthal, and P. Andolfatto. 2014. High-
578 resolution mapping reveals hundreds of genetic incompatibilities in hybridizing fish
579 species. Elife 3:e02535.
580 Simon, A., N. Bierne, and J. J. Welch. 2017. Coadapted genomes and selection on hybrids:
581 Fisher's geometric model explains a variety of empirical patterns. bioRxiv, doi:
582 https://doi.org/10.1101/237925.
583 Slatkin, M., and R. Lande. 1994. Segregation variance after hybridization of isolated
584 populations. Genet. Res. 64:51–56.
585 Stearns, F. W., and C. B. Fenster. 2016. Fisher's geometric model predicts the effects of random
586 mutations when tested in the wild. Evolution 70:495–501.
587 Stuart, Y. E., T. Veen, J. N. Weber, D. Hanson, M. Ravinet, B. K. Lohman, C. J. Thompson, T.
588 Tasneem, A. Doggett, R. Izen, N. Ahmed, R. D. H. Barrett, A. P. Hendry, C. L. Peichel, and D.
589 I. Bolnick. 2017. Contrasting effects of environment and genetics generate a continuum of
590 parallel evolution. Nat. Ecol. Evol. 1:0158.
591 Tenaillon, O. 2014. The utility of Fisher's geometric model in revolutionary genetics. Annu. Rev.
592 Ecol. Evol. Syst. 45:179–201.
593 Weir, J. T., and D. Schluter. 2004. Ice sheets promote speciation in boreal birds. Proc. R. Soc. B
594 Biol. Sci. 271:1881–1887.
595 Wright, S. 1968. Evolution and the Genetics of Populations Vol. 1. Genetic and Biometric
596 Foundations. University of Chicago Press, Chicago, IL.
597

598 **Table 1.** Description of parameters in adapting populations.

Parameter	Value
B, number of offspring produced by each mating (# individuals)	2
d, distance to the optimum	$0.2 \leq d \leq 1$
K, carrying capacity (# individuals)	1000
m, number of traits, or 'dimensionality'	2
n, number of alleles in the standing variation	0 - 150
σ, mutation size SD	0.1
p, probability that a mutation is present in an individual ancestor	0.1
μ, probability an individual acquires a new mutation	0.001
s, strength of selection	1
Θ, angle of divergence (°)	$0 \leq \Theta \leq 180$

599

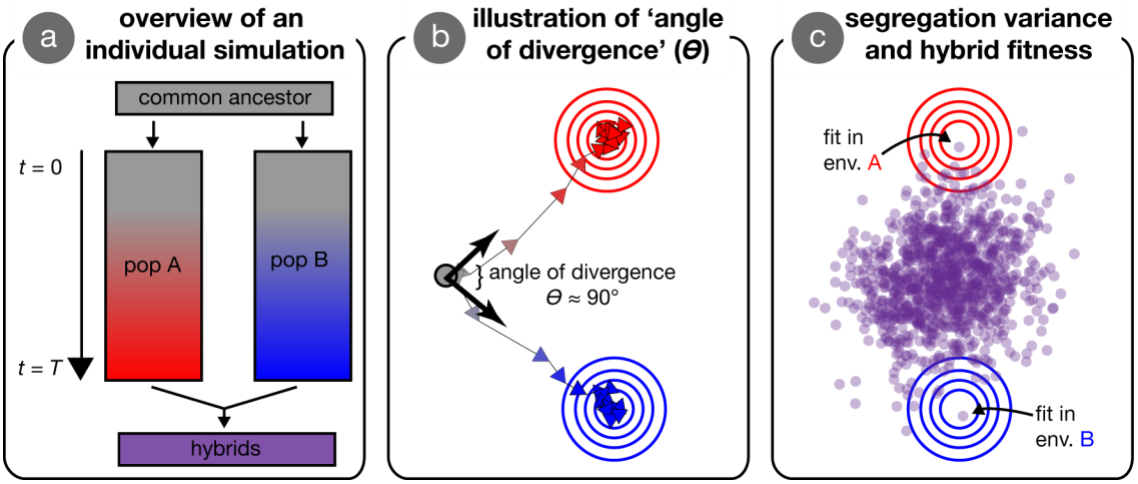

Figure 1. Visual overview of simulations and concepts. Panel (a) provides an overview of an individual simulation. An ancestral population founds two initially-identical populations, that evolve independently for *T* generations in their respective environments. After *T* generations of adaptation, these derived populations interbreed to form hybrids. Panel (b) illustrates the process of adaptation in our simulations, wherein two populations (red and blue arrows) independently adapt to specified optima. Concentric circles represent fitness contours around the two optima, with the peaks at the centres. The ancestor state is indicated by the grey dot, with the angle of divergence, Θ, shown between the two directions of selection (black arrows; angle shown is approximately 90°. Panel (c) illustrates the segregation variance in a group of hybrids. Individual hybrids that are nearer an optimum have higher fitness when measured in that environment.

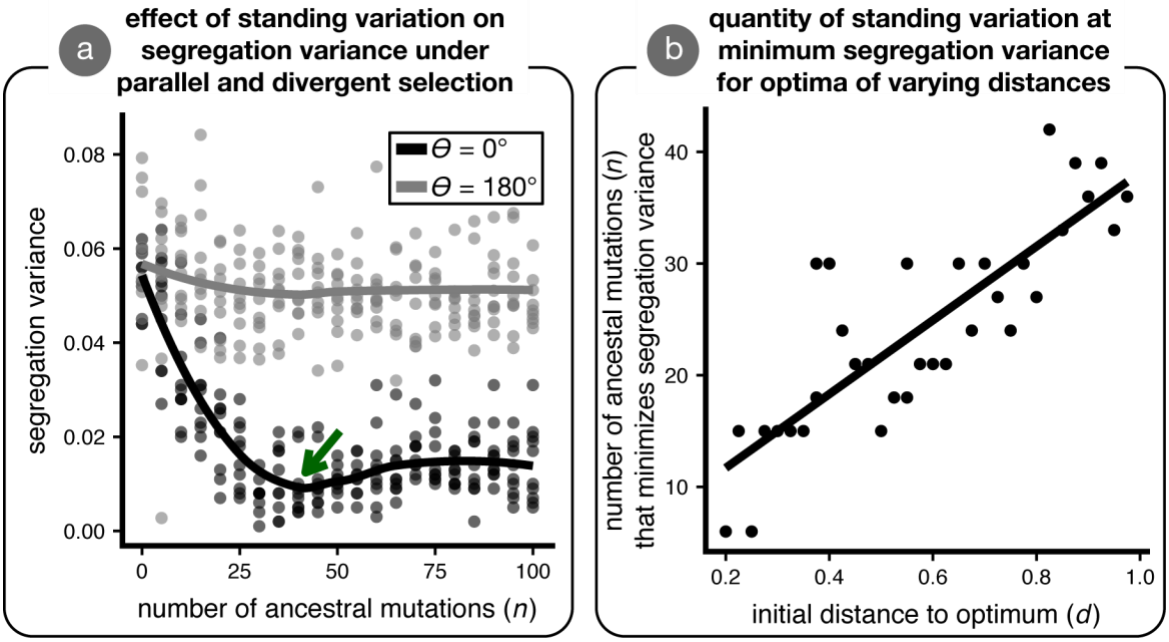

Figure 2. The effects of standing genetic variation on segregation variance in hybrids under parallel and divergent natural selection. Panel (a) shows values of segregation variance observed in 10 simulations for both parallel (Θ = 0°; black) and divergent (Θ = 180°; grey) selection for populations founded with varying quantities of ancestral standing variation (number of ancestral mutations). The green arrow indicates the value of n with the lowest median segregation variance. The curves are loess fits. Distance between the ancestor state and each optimum is d = 1. Panel (b) shows that the quantity of ancestral standing variation that minimizes segregation variance under parallel selection (Θ = 0°) increases when populations adapt to more distant optima. The line is a linear regression.

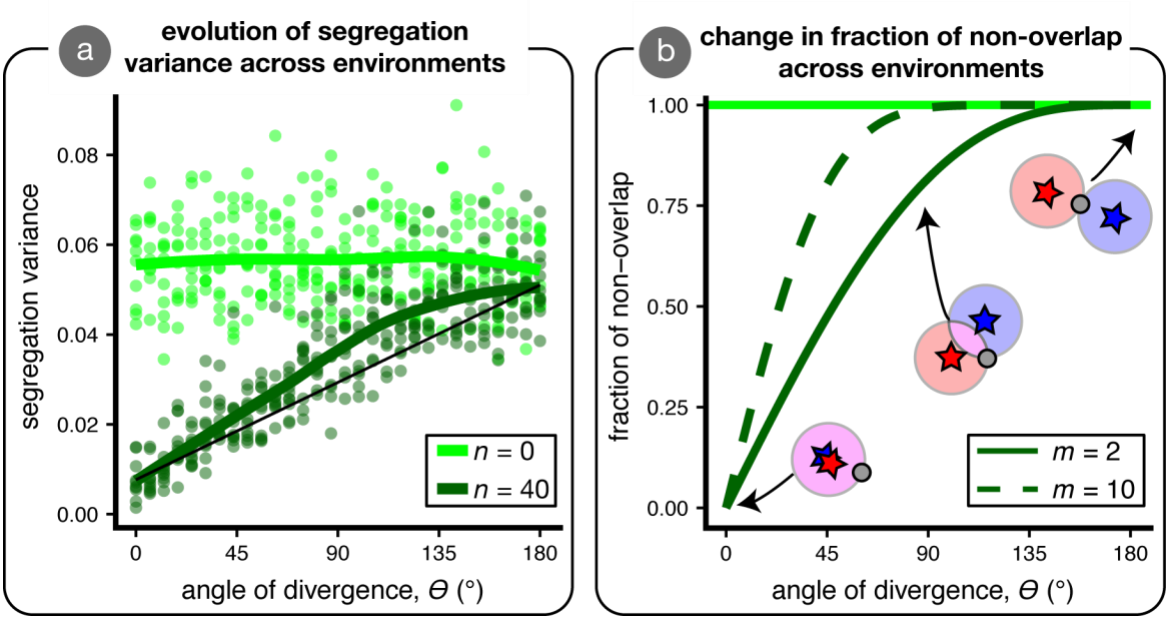

Figure 3. Segregation variance and non-parallel evolution across environments. We conducted simulations for optima separated by different angles (Θ = 0° to 180°; d = 1) and measured the resulting segregation variance in hybrids over 10 replicates. Panel (a) plots two cases of standing variation: no standing variation (n = 0; light green) and the amount of standing variation that minimizes segregation variance at Θ = 0° (n = 40; dark green). Curves are loess fits. Panel (b) depicts the relationship between the initial fraction of mutations that are beneficial in one population but deleterious in the other population for two different dimensionalities (m =2 [solid line] & 10 [dashed line]). In the inset cartoon, mutations in the red and blue regions are initially beneficial only in the 'red' or 'blue' environments, while mutations in the pink region are mutually beneficial (i.e., the red area divided by the pink and red area together is the fraction of non-overlap). The horizontal light green line is set at 1 where there is complete non-overlap.

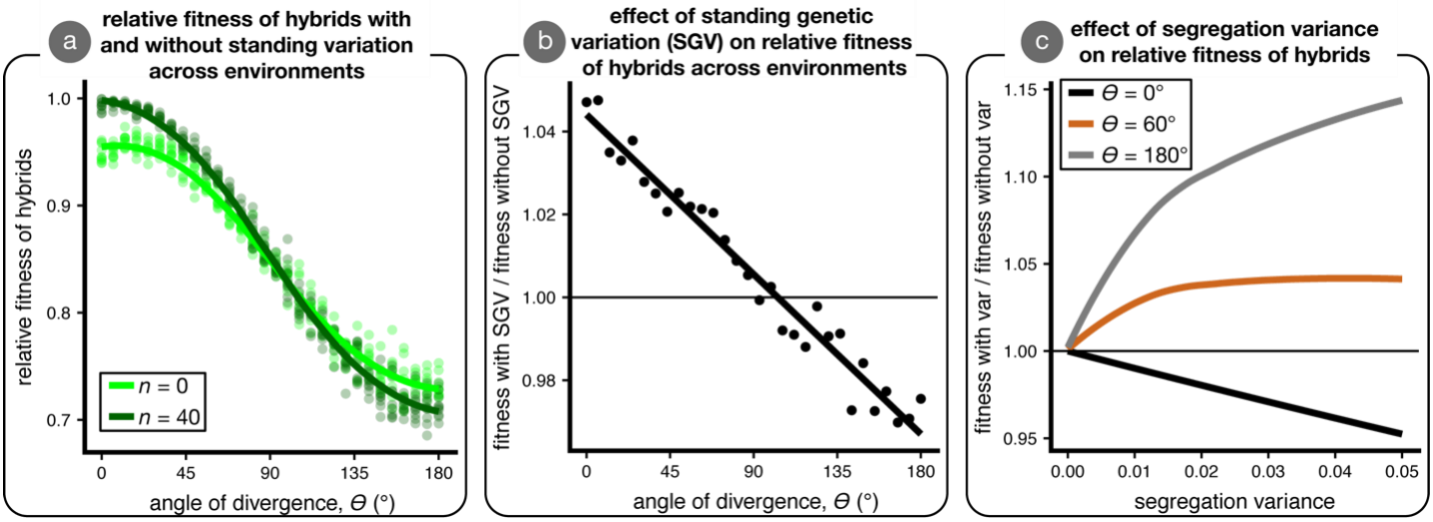

Figure 4. The effect of standing variation on mean hybrid fitness. Panel (a) shows the mean relative fitness of hybrids—as compared to parents—across environments in simulations initiated without (n = 0; light green) and with (n = 40; dark green) ancestral standing genetic variation. Panel (b) shows the effect of standing variation on mean relative hybrid fitness (the ratio of values for dark: light green lines in panel [a]); the horizontal line indicates no effect of standing variation on relative mean hybrid fitness. Panel (c) illustrates the relationship between segregation variance and mean hybrid fitness for three values of angle Θ (black, Θ = 0°; brown, Θ = 60°; grey, Θ = 180°) hybrid phenotypes are assumed to be multivariate normal with mean between the two parental optima and equal variance in all phenotypic dimensions (no covariance). Hybrid fitness is plotted for each angle relative to the case of no variance; the horizontal line indicates that segregation variance has no effect on hybrid fitness. The data in panels (a) and (b) are from the simulations plotted in Fig. 3A.

651 **Supporting information for:**

652 **Patterns of speciation and parallel genetic adaptation from standing variation**

653 **by**

654 **Ken A. Thompson, Matthew M. Osmond and Dolph Schluter**

655

656 **Contents:**

657 Appendix 1

658 Figures S1-6.

659

Appendix 1

Here we outline an explanation for why segregation variance increases faster-than-linearly with the angle of divergence, Θ (Fig. 3A). In our simulations, non-zero segregation variance after hybridization can only arise from non-parallel genetic evolution in the parental populations. Therefore, this explanation is equivalent to explaining why the extent of non-parallel genetic adaptation increases faster-than-linearly with the angle of divergence.

Our explanation focuses on the extent of phenotypic space wherein mutations are mutually beneficial, that is, improve the fitness both adapting populations in their respective environments. At the time of founding both adapting populations are expected to have the same mean phenotype, which is the mean ancestral phenotype. Mutations that move this ancestral mean phenotype into the region that has higher fitness in both parental environments are thus mutually beneficial (at least when phenotypes are sufficiently clustered around the mean). The region of phenotypic space that has higher fitness than the mean in one environment is a hypersphere (of dimension m), centered on the optimum with a radius equal to the distance between the mean phenotype and the optimum, d. A second hypersphere describes the phenotypic space that has higher fitness than the mean phenotype in the other parental environment. The region that is mutually beneficial is then the intersection of two hyperspheres, which is the union of two hyperspherical caps.

Fortunately, the volume of a hyperspherical cap is known for any dimension, m (Li 2011). It depends on the dimensionality, the radii of the two hyperspheres, and the distance between their centers. In our case the radii are equivalent and equal to d and the distance between the two centres is $\delta = d\,[2(1 - \mathrm{Cos}\Theta)]^{1/2}$. Thus, the amount of phenotypic space that is

mutually beneficial can be written as a function of m, d, and Θ. The amount of phenotypic space that is beneficial in a given environment is simply the volume of one of the hyperspheres. Dividing the volume of the mutually-beneficial space by the volume of the space beneficial in a given environment gives the fraction of beneficial mutations which are mutually beneficial

$$I_x[(1 + m)/2, 1/2] \quad \text{(A1)}$$

where $I_x[a, b]$ is the regularized incomplete beta function (Equation 6.6.2 in Abramowitz and Stegun [1972]) and here $x = \text{Cos}(\Theta/2)^2$. Eq. A1 depends on only m and Θ, i.e., it is independent of the distance from the ancestor to the new optima, d. We refer to Eq. A1 as the fraction of overlap, and one minus Eq. A1 as the fraction of non-overlap.

The fraction of non-overlap (one minus Eq. A1) exhibits a faster-than-linear increase with Θ for all values of $m > 0$, and the increase is faster for greater values of m (Fig. 3B). Thus, if standing genetic variation was uniformly distributed throughout the beneficial hyperspheres, the percent of segregating beneficial mutations that were beneficial, and thus expected to fix, in only one adapting population would increase faster-than-linearly with the angle of divergence.

The above analysis considers only the very onset of adaptation, when the two adapting populations have the same mean phenotypes, such that the fraction of phenotypic space that is beneficial in one population that is also beneficial in the other population (call this X) is equivalent to the fraction of beneficial mutations (if uniformly distributed across the hyperspheres) that are mutually beneficial (call this Y). As adaptation proceeds the mean phenotypes of the adapting populations depart from one another and X therefore no longer equals Y. This is because mutations are vectors that move a phenotype in a particular direction,

and thus a mutually beneficial point in phenotypic space is only a mutually beneficial mutation if both populations have the same mean phenotype. To see this, imagine two populations whose mean phenotypes begin at the origin but move towards (1,0) and (0,1) respectively. As these populations adapt and depart from the origin along the x and y axes, there remains for some time a fraction of mutually beneficial phenotypic space (*X*) around the line x=y between the two optima. But a mutation that moves the (1,0) population into this space is a vector pointing primarily right, while a mutation that moves the (0,1) population into this same space is a vector pointing primarily up. Another way to see that *X* does not equal *Y* is to consider what happens as these two populations approach their optima. The fraction of mutually beneficial space then approaches zero, yet very sufficiently small mutations that move phenotypes up and to the right are mutually beneficial.

To account for the inequality between phenotypic space (*X*) and mutational vectors (*Y*) during adaptation we must shift the mean phenotypes so that they are at the same point in phenotypic space, and move their optima by an identical translation. We then have *X*=*Y*. An easy way to imagine this is to keep the mean phenotypes in place at the mean ancestral phenotype (the origin) and consider adaptation as the movement of the optima closer to the mean phenotypes (i.e., the difference between the optimal and current phenotype). From this perspective, as adaptation proceeds the radii of the hyperspheres shrinks (roughly equivalently in the two populations) but there remains some region of overlap. In fact, because the fraction of overlap (Eq. A1) does not depend on the radii of the hyperspheres, the fraction of non-overlap is expected to remain constant throughout adaptation as long as Θ is constant.

In reality and in our simulations, standing genetic variation is not uniformly distributed, the probability of fixation varies across the region of overlap, and adaptation uses up some of the standing variation so that the distribution of standing variation changes with time. Taking the first two complications into account would require weighted averages across the space contained in the hyperspherical caps, which is beyond the scope of our study. The third complication is yet more involved, and would require an analysis of how standing genetic variation is used as adaptation proceeds (i.e., how the distribution of segregating effects and allele frequencies shift as alleles fix). Such a calculation is also beyond the scope of this article. Despite these complications, it seems that the simple analysis above qualitatively captures the essence of why segregation variance increases faster-than-linearly with the angle of divergence.

735 **Supplementary figures**

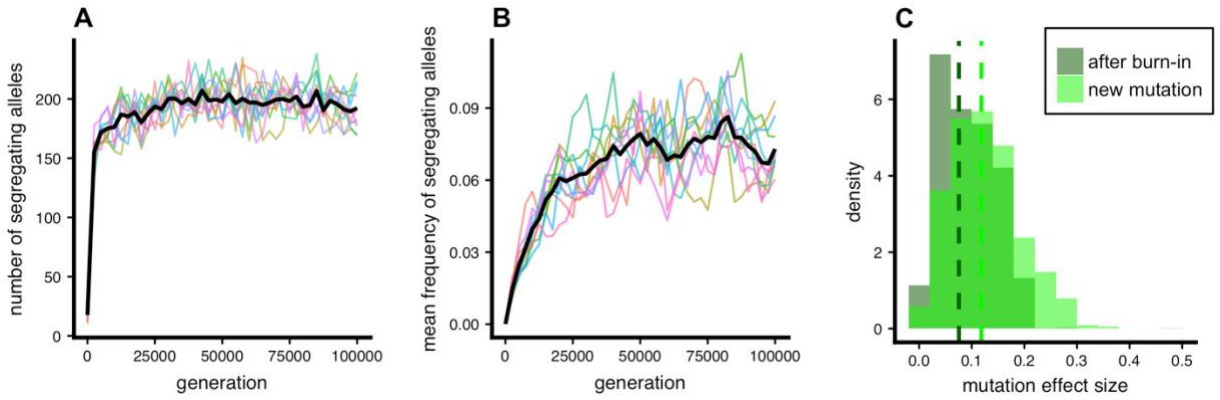

736

737 **Fig. S1. Mutation-selection balance and mutation effect sizes in ancestral populations.** (a) The
738 number of segregating (i.e., unfixed) alleles in each of 10 ancestral populations and (b) the
739 mean frequency of such alleles in the ancestral populations. The black line is plotted through
740 the mean of all populations at each generation, and all ten burn-ins used to generate our
741 results are shown. Panel (c) illustrates the distribution of mutation effect sizes at the end of a
742 single burn-in simulation, as compared to the distribution of mutations that arise *de novo*. The
743 vertical lines represent the median mutation effect size for each group.

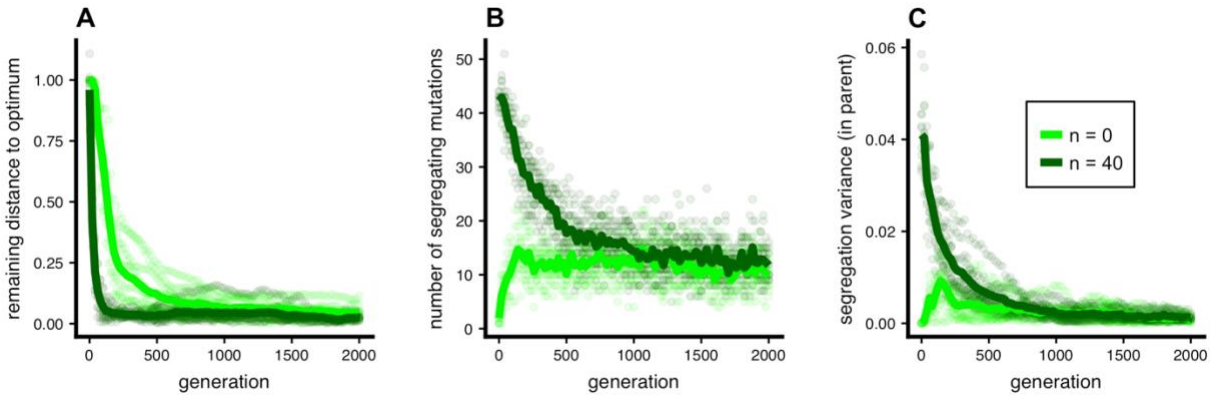

744

745 **Fig. S2. Effect of standing variation on the pace of adaptation and attainment of mutation**

746 **selection-balance.** (a) Populations that adapt with standing variation in addition to new

747 mutation (*n* = 40 mutations; dark green) reach the phenotypic optimum more quickly than

748 populations that adapt from new mutation only (*n* = 0; light green). (b) Although populations

749 equipped with standing variation adapt more quickly than populations adapting from new

750 mutation only, they both reach mutation-selection balance by generation 2000. (c) The

751 segregation variance in parental populations, calculated as it is in hybrids (see main text), is

752 stable and near zero by the end of each simulation. The initial distance to the optima, *d*, is 1 for

753 all simulations. We plot 10 replicate simulations, and lines connect the mean values at each

754 sampled generation.

755

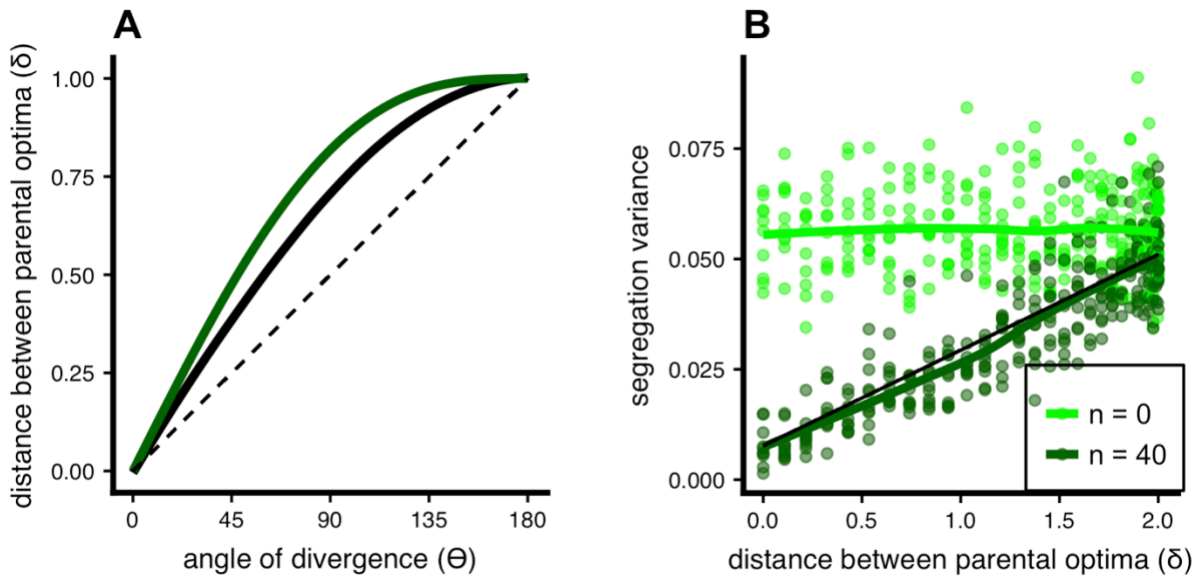

Fig. S3. Alternative presentation of simulation results across environments: distance between optima (δ). Panel (a) plots the relationship between the angle of divergence, Θ, and the Euclidean distance between parental optima, δ (thick black line). We also plot the fraction of beneficial mutations expected to be beneficial in just one population (fraction of non-overlap) for m = 2 (dark green line; see Fig. 3B). The dashed black line is the 1:1. Panel (b) plots the same data in as in Fig. 3A, respectively, but with δ on the x-axis. In higher dimensions δ is constant and so the faster-than-linear pattern emerges even when considering δ.

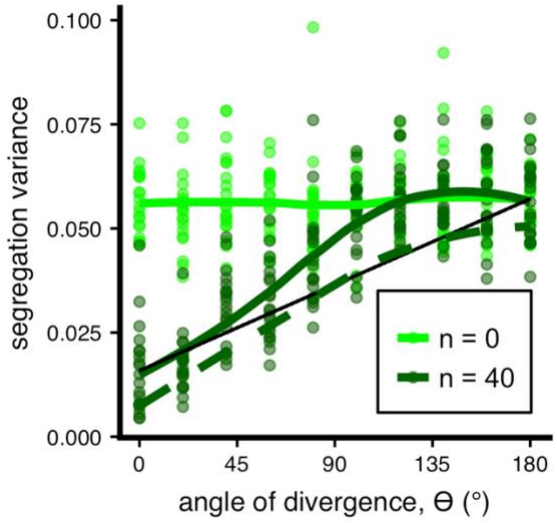

765

766 **Fig. S4. Segregation variance with standing variation generated from mutation-distribution**

767 **rather than a burn-in.** We generated standing variation from the raw mutation distribution,

768 such that mutations in the standing variation have identical properties to those arising *de novo*

769 (i.e., before selection). The dashed dark green line is the loess fit from simulations where the

770 standing variation was generated from a burn-in using the same data as from Fig. 3A in the

771 main text. Segregation variance is equivalent for simulations initiated with and without

772 standing variation from the mutation-distribution for large angles, indicating that populations

773 fix alternative mutations from this standing variation and that the properties of the mutations

774 fixed with and without this standing variation are similar. For all simulations, the initial distance

775 to the optimum, *d* was 1, and the initial frequency of mutations was 10 %.

776

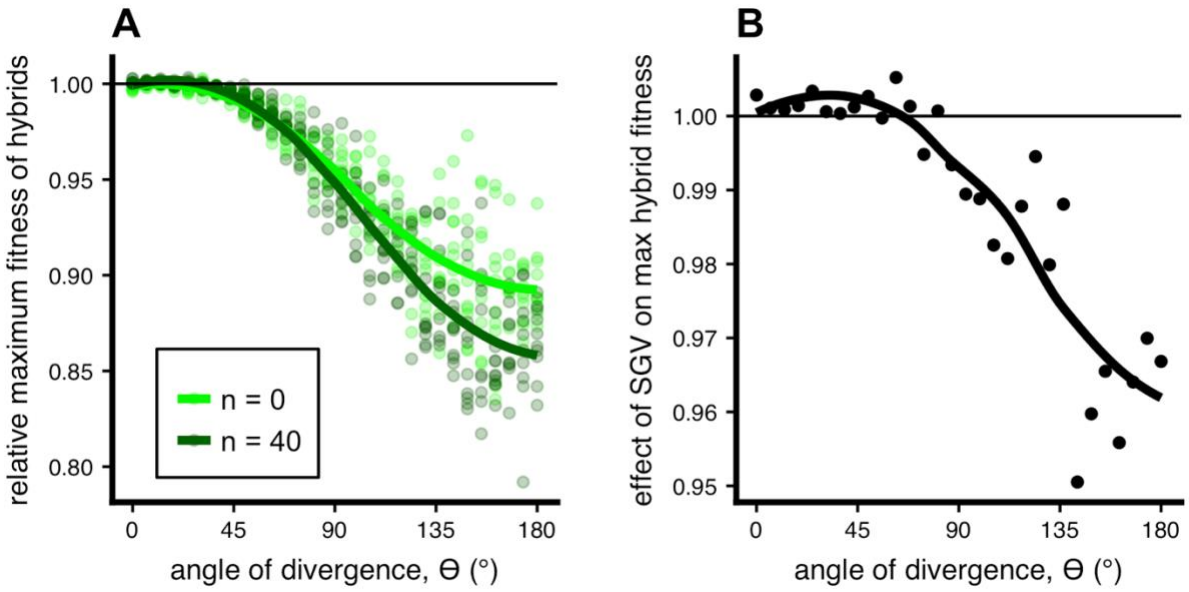

Figure S5. The effect of standing genetic variation (SGV) on maximum hybrid fitness across environments. Data are identical to that plotted in Fig. 3A and 4A & B of the main text, but instead of mean fitness we depict the relative fitness of top 5 % of hybrids to all parents. This is calculated as [mean probability of survival for the 5 % of hybrids with highest probability] / [mean probability of survival for parents]. We plot both the (a) raw values of relative maximum fitness and (b) the effect of standing variation on maximum hybrid fitness (dark green divided by light green). There is not much of an effect of standing variation on maximum hybrid fitness under parallel natural selection, but quite a negative effect under divergent selection.

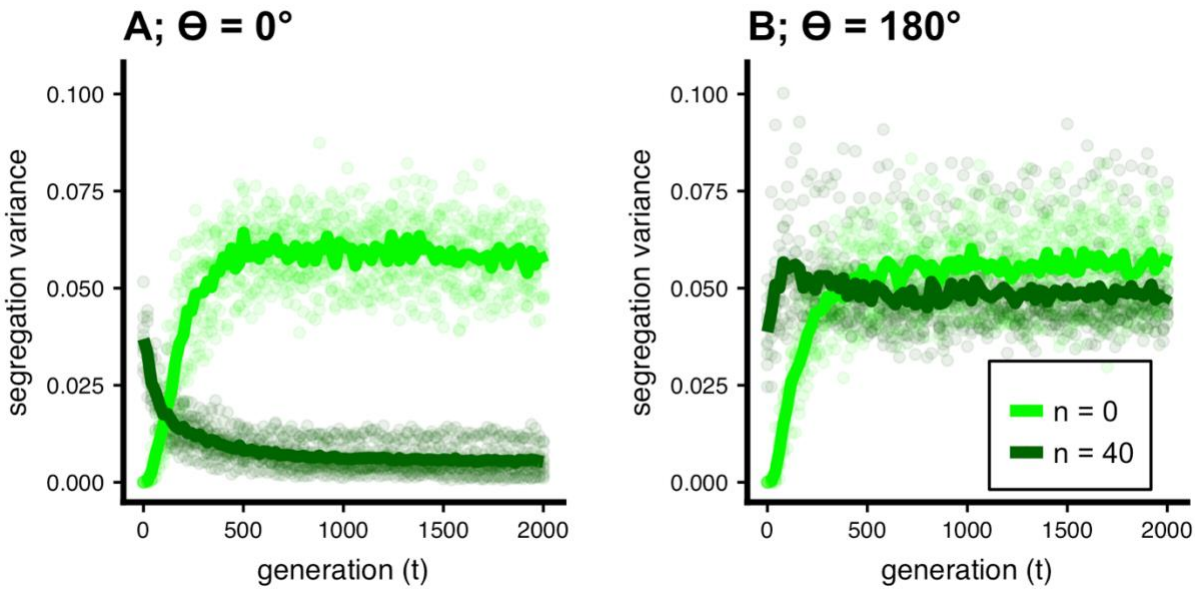

787

788 **Fig. S6. Evolution of segregation variance over time with and without standing variation.** We

789 depict two scenarios, (A) parallel (Θ = 0°) and (B) divergent (Θ = 180°) for m = 2 and d = 1. We

790 plot segregation variance, a component of hybrid fitness, measured every 100 generations over

791 the course of the adaptive walk. We plot 10 replicate simulations, and lines are drawn through

792 the mean value at each sampled generation.

793